12-1-2022

Chromophoric Dissolved Organic Matter and Dissolved Organic Carbon in Lakes Across an Elevational Gradient From the Mountains to the Sea

Kyle Juetten
Western Washington University

Angela Lee Strecker
Western Washington University

Aaron Harrison
Austin College

Zachary Landram
Western Washington University

Warren J. De Bruyn
Chapman University

See next page for additional authors

Recommended Citation

Juetten, K., Strecker, A. L., Harrison, A., Landram, Z., De Bruyn, W. J., & Clark, C. D. (2022). Chromophoric dissolved organic matter and dissolved organic carbon in lakes across an elevational gradient from the mountains to the sea. Earth and Space Science, 9, e2022EA002503. https://doi.org/10.1029/2022EA002503

ADVANCING EARTH AND SPACE SCIENCE

Earth and Space Science

RESEARCH ARTICLE
10.1029/2022EA002503

Key Points:

- Dissolved organic carbon and chromophoric dissolved organic matter amounts decrease in lakes at higher elevations with lower wetland and agricultural land cover
- Most lakes are dominated by allochthonous terrestrial material, with more aromatic humified material at lower elevations
- Relative contribution of autochthonous material is more important at higher elevations, possibly due to shifts in vegetation types

Supporting Information:

Supporting Information may be found in the online version of this article.

Correspondence to:

C. D. Clark,
Catherine.Clark@wwu.edu

Citation:

Juetten, K., Strecker, A. L., Harrison, A., Landram, Z., De Bruyn, W. J., & Clark, C. D. (2022). Chromophoric dissolved organic matter and dissolved organic carbon in lakes across an elevational gradient from the mountains to the sea. *Earth and Space Science*, *9*, e2022EA002503. https://doi.org/10.1029/2022EA002503

Received 13 JUL 2022
Accepted 22 NOV 2022

Author Contributions:

Conceptualization: Catherine D. Clark
Formal analysis: Angela L. Strecker, Aaron Harrison, Warren J. De Bruyn
Investigation: Kyle Juetten, Zachary Landram
Methodology: Catherine D. Clark

Chromophoric Dissolved Organic Matter and Dissolved Organic Carbon in Lakes Across an Elevational Gradient From the Mountains to the Sea

Kyle Juetten[1], Angela L. Strecker[2,3], Aaron Harrison[4], Zachary Landram[1], Warren J. De Bruyn[5], and Catherine D. Clark[1]

[1]Department of Chemistry, College of Science and Engineering, Western Washington University, Bellingham, WA, USA, [2]Institute for Watershed Studies, College of the Environment, Western Washington University, Bellingham, WA, USA, [3]Department of Environmental Sciences, College of the Environment, Western Washington University, Bellingham, WA, USA, [4]Department of Chemistry, Austin College, Sherman, TX, USA, [5]Chemistry and Biochemistry Program, Schmid College of Science and Technology, Chapman University, Orange, CA, USA

Abstract Dissolved organic matter (DOM) in lakes across elevation gradients is a complex function of topography, climate, vegetation coverage, land use, and lake properties. To examine sources and processing of DOM from sea level to mountain lakes (3–1,574 m), we measured dissolved organic carbon (DOC) concentrations and chromophoric dissolved organic matter (CDOM) optical properties, lake characteristics, and water quality parameters in 62 freshwater lakes in the Pacific Northwest, USA. Higher elevation lakes had lower DOC concentrations and absorbance. These lakes had higher forest cover and minimal wetlands in their watershed, in addition to low nutrients, water temperatures, and chlorophyll *a* in the lake itself. Two humic-like and one protein-like fluorescent component were identified from excitation-emission matrix spectroscopy. The index of recent autochthonous contribution (BIX), fluorescence index (FIX), and S_R optical indices showed that most lakes were dominated by terrestrially derived material. The humification index (HIX) and specific ultra-violet absorbance (SUVA254) were consistent with more aromatic humic CDOM at lower elevations. The lower fluorescence of humic-like components at higher elevation was attributed to lower inputs from vegetation. The relative contribution of the protein-like component increased at higher elevation. This may be due to reduced allochthonous terrestrial inputs relative to in situ production of autochthonous material or increased photochemical/biological degradation of allochthonous material. Differences in optical characteristics associated with the amount and source of CDOM were observed across the elevational gradient. These differences were driven by characteristics at both within-lake and watershed scales.

Plain Language Summary Dissolved organic matter (DOM) in lakes is an important part of the global carbon cycle. The amounts, sources, and properties of DOM can vary as a function of lake elevation due to changes in vegetation, lake properties, climate, and topography. To assess these patterns, we studied DOM in 62 lakes ranging from sea level to mountain lakes in the Pacific Northwest region of the USA. Lower elevation lakes had higher levels of DOM, attributed to higher inputs from the terrestrial environment. Higher elevation lakes had lower wetland coverage within their watershed. Results also indicated that some lakes had DOM that came from microbial production in the lake waters. This was more important in higher elevation lakes that had lower amounts of DOM from vegetation in the watershed. Differences in DOM amount and source were observed across the elevational gradient, driven by an interplay of characteristics at both within-lake and watershed scales.

1. Introduction

Lakes play an important role in global carbon cycling (Tranvik et al., 2009). Carbon inputs from the surrounding watershed and in situ production from microorganisms are processed in lake waters. Dissolved organic matter (DOM), a part of the carbon pool in aquatic ecosystems, consists of very large water-soluble organic molecules with complex structures that include aromatic and aliphatic moieties (Minor et al., 2014; Nebbioso & Piccolo, 2013). DOM plays a substantial role in lake food webs, stimulating bacterial production and ultimately, biomass of upper trophic levels (Creed et al., 2018). Carbon is transformed in lakes via photolysis (Molot & Dillon, 1997), the biological and photochemical processing of DOM (Li et al., 2022), biological processes like decomposition and respiration (Urban et al., 2005), and physical processes like flocculation and selective sorption

Project Administration: Catherine D. Clark
Resources: Catherine D. Clark
Supervision: Catherine D. Clark
Visualization: Kyle Juetten, Angela L. Strecker, Aaron Harrison, Warren J. De Bruyn, Catherine D. Clark
Writing – original draft: Kyle Juetten, Catherine D. Clark
Writing – review & editing: Angela L. Strecker, Warren J. De Bruyn, Catherine D. Clark

into sediments as a carbon sink (von Wachenfeldt et al., 2008). Mineralization processes that convert DOM to carbon dioxide and volatile organic carbon species can be a significant source of carbon to the atmosphere (Allesson et al., 2021; Obernosterer & Benner, 2004). These photochemical, physical, and biological processes affect DOMs molecular characteristics and bioavailability (Moran & Zepp, 1997; Obernosterer & Benner, 2004) and produce a range of reactive transient species and small organic compounds that impact aquatic biogeochemical cycles (Vione et al., 2014).

Chromophoric dissolved organic matter (CDOM) is the light-absorbing component of DOM (Green & Blough, 1994). CDOM in lakes is primarily of allochthonous origin from soils and terrestrial plants, with some influence of autochthonous material from microorganisms (McKnight & Aiken, 1998) or macrophytes (Clark et al., 2020; He et al., 2018; Vila Dupla, 2022; Wang et al., 2014). There are also contributions from the alteration of terrigenous material by biological and photochemical processing (Urban et al., 2005). CDOMs optical properties have been used to differentiate between allochthonous and autochthonous sources and track biological and photochemical transformations of DOM (Hessen & Tranvik, 1998; Zhang et al., 2021). For example, DOM fluorescence has been used to determine the sources and transport of DOM in coastal waters (Stedmon et al., 2003) and has been shown to vary with surrounding land cover for lakes (Song, Li, et al., 2019; Song, Shang, et al., 2019; Zhao et al., 2017). CDOM has been shown to be a reliable, regional proxy for DOC in lakes where forests and wetlands dominate the catchment and DOM is primarily terrestrial in origin (Griffin et al., 2018). However, some recent work has shown some decoupling between CDOM and DOM increases in Swedish waterways over decadal timescales (Eklof et al., 2021).

The overall amount of CDOM in lakes, the relative contribution from allochthonous versus autochthonous material, and the degree of processing are a complex function of regional topography, watershed size, local land use and vegetation, chemical properties, nutrient runoff and associated biological properties of the lake, season, and regional climate. For example, lakes at high elevation with reduced vegetation coverage in the watershed compared to lower elevation lakes would be expected to have lower allochthonous inputs from terrestrial material. If allochthonous material is the dominant source of CDOM, decreasing CDOM with elevation will also likely have an impact on lake photic depth, which will in turn impact in situ biological production of autochthonous material and photochemical and biological processing of CDOM. Watersheds dominated by agriculture are likely to have higher nutrient runoff, which may increase phytoplankton concentrations and hence biological production of autochthonous material. A number of these variables that control CDOM in lakes are also climate sensitive; this is particularly true in mountain regions. For example, climate change will likely shift the treeline and the types of vegetation found at different elevations in mountain ecosystems, which will change the inputs and cycling of CDOM in these systems (Olson et al., 2021). CDOM concentrations could also change with warming temperatures due to increased microbial respiration or increased production from phytoplankton (Thornton, 2014).

A number of studies have examined CDOM optical properties in lakes across elevation gradients. These studies are starting to provide regional reference points that will help constrain predictions of future changes in carbon flow in these areas as climate shifts. Given the climate sensitivity of alpine regions and the treeline, most have focused on lakes in high elevation regions (De Laurentiis et al., 2012; Laurion et al., 2000; Olson et al., 2021; Rose et al., 2015; Song, Li, et al., 2019; Song, Shang, et al., 2019; Su et al., 2015; Zhang et al., 2010) or lower elevation sub-Arctic regions that also include lakes above and below the treeline (Arvola et al., 2016; Rantala et al., 2016). In most of these studies, there were changes in allochthonous inputs to lakes across the treeline. However, shifts in vegetation coverage and land use across all elevational gradients will likely affect CDOM inputs and processing in lakes.

To elucidate trends in DOM sources and processing across an elevational gradient, we measured DOC concentrations and the optical properties of CDOM across 62 lakes in the Pacific Northwest region in Washington State, USA, ranging from 3 to 1,574 m above sea level. We are unaware of any reported studies on CDOM across a similar elevational gradient covering sea level to mountain lakes. Our study focuses on DOC and CDOM changes as a function of elevation, land use/land cover, vegetation type, and lake characteristics. A range of optical properties of CDOM, watershed characteristics (like watershed area, vegetation type, and coverage), and water quality parameters were measured for each lake. Ours is the first study of CDOM optical properties in lakes in the Pacific Northwest region of the USA and adds to the current knowledge of CDOM across elevational gradients and as a function of types of land cover.

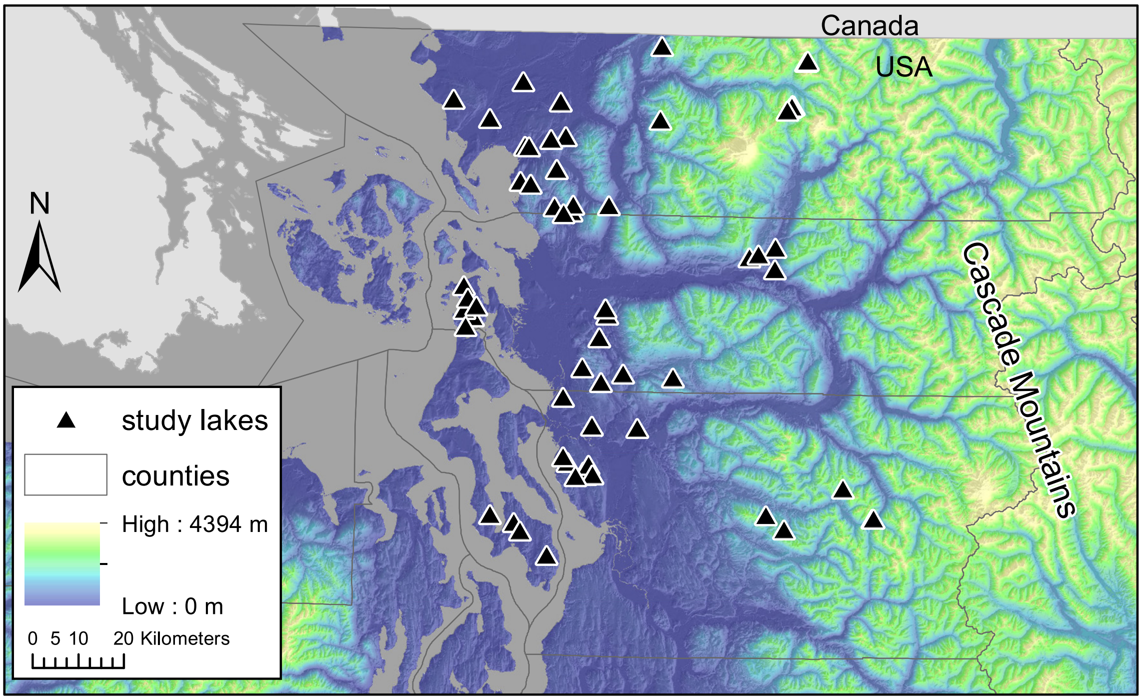

Figure 1. Map of Pacific Northwest lakes sampled in 2018. Lake coordinates and sampling dates are provided in Table S1 in Supporting Information S1 (Juetten et al., 2022; https://doi.org/10.25710/6x7v-4858). The dark gray areas are the waters of the Salish Sea, while gray lines represent county or international borders.

2. Materials and Methods

2.1. Site Description

We sampled 62 lakes in northeastern Washington State, USA from June 25 to August 29, 2018 (Table S1 in Supporting Information S1; Juetten et al., 2022; https://doi.org/10.25710/6x7v-4858). The lakes included are part of Western Washington University's Institute for Watershed Studies Northwest Lake Monitoring program and are located in Whatcom, Snohomish, Skagit, and Island counties, ranging from urban to undeveloped surroundings (Figure 1). Each lake is briefly described on the Institute's website (https://diatom.cenv.wwu.edu/?page=lakeslist). Study lakes span a wide range of elevations (3–1,574 m above sea level), human population densities, surface areas (1.2–833.7 ha, median = 24.0 ha), and trophic status (oligotrophic to hypereutrophic) (Table 1). Most of the lakes are natural, but at least one reservoir is included in our study (Lake Shannon). None of the lakes have

Table 1
Summary of the Physical and Landscape Characteristics of the Lakes in the Study

Parameter	Minimum	Maximum	Median
Surface area (ha)	0.4	833.7	12.8
Elevation (m)	3.0	1,574.0	123.0
Watershed area (ha)	0.5	76,383.3	210.0
% Developed	0.1	58.1	10.6
% Forest (deciduous + evergreen + mixed)	1.4	94.6	62.9
% Herbaceous + shrub	0.0	58.2	4.5
% Agriculture (pasture + cultivated crop)	0.0	68.0	0.4
% Wetland	0.0	42.8	1.1
% Total vegetation	34.6	98.7	77.9

Note. Data for individual lakes are provided in Table S1 in Supporting Information S1 (Juetten et al., 2022; https://doi.org/10.25710/6x7v-4858). Land cover is within each lake's watershed.

glaciers within their watersheds. Many of the higher elevation lakes studied here are in the Mt. Baker-Snoqualmie National Forest (including nine in a Research Natural Area, designated as a federal protected area) with limited human activity in the watershed; the relative amount of the watersheds that are covered by agriculture is essentially zero above about 500 m.

High elevation lakes are primarily located in the Cascade Mountains, in the eastern part of the study region (Figure 1). There are also some high elevation lakes located in the Chuckanut Mountain coastal range in the northwestern region. Watersheds were delineated in ArcGIS 10.7.1 using 30-m digital elevation models (United States Geological Survey, 2020) and ranged from 0.5 to 76,383.3 ha (Table 1). Here, watershed is defined as the entire upstream land surface that drains to a specific point (i.e., the lake outlet), combining all upstream catchments following the definition and usage of Hill et al. (2018). Each lake has a unique watershed. Land cover classifications within watersheds were obtained from the 2019 National Land Cover Database (Dewitz and U.S Geological Survey, 2021). Watershed land cover varied, with a range of different vegetation types (forested, herbaceous and shrubs, wetland) and development (urban and agriculture) (Table 1 and Figure S1 in Supporting Information S1).

2.2. Sampling

Lake water was collected in amber glass bottles from the shoreline at public access points using a sample bottle attached to a long pole to avoid disturbing the sediment. Samples were filtered through Durapore 0.22-μm PVDF membrane filters to remove debris and microorganisms before measuring optical properties. Samples were stored in glass bottles in the dark at 4°C for at most 2 days before optical analysis.

2.3. Water Quality Measurements

A YSI EXO1 multiparameter field meter was used to measure temperature, pH, dissolved oxygen, and specific conductance in situ. The YSI was deployed from the shoreline. Water samples were analyzed for alkalinity, turbidity, chlorophyll *a* (as a proxy of phytoplankton biomass), total nitrogen (TN), and total phosphorus (TP) by the Institute for Watershed Studies using standard methods (APHA, 1989; EPA, 1983). TN and TP were analyzed on an OI Analytical FS3100 Flow Injection Analyzer, with method detection limits (MDL) of 0.1 mg N L^{-1} and 0.005 mg P L^{-1}. Relationships between water quality variables were analyzed with a Pearson correlation test and visualized with the R library *corrplot* (v. 0.92). Analyses were run in R v. 4.0.3 (R Core Team, 2020) with R Studio v. 2022.02.0.

2.4. Dissolved Organic Carbon

DOC concentrations (mg L^{-1}) were measured with a TOC analyzer (Shimadzu Inc.). The instrument has a method detection limit (MDL) of 0.20 mg C L^{-1} and a minimum reporting level (MRL) of 0.34 mg C L^{-1}. Samples were acidified to pH < 2 with 6 M hydrochloric acid and stored at 4°C in 50-ml glass DOC vials with Teflon-lined caps for no more than 30 days before analysis.

2.5. Fluorescence

Excitation-emission matrices (EEMs) were acquired using an Aqualog spectrofluorometer (HORIBA Scientific Inc.) in uncapped quartz fluorescence cells with a 1-cm path length. The instrument has a wavelength accuracy of ±1 nm and an effective analysis range from 230 to 800 nm. The light source is a 150-W ozone-free xenon arc lamp. The Aqualog uses a TE-cooled CCD fluorescence emission detector which allows for ultrafast simultaneous measurement of absorbance and fluorescence. Instrument software corrects for inner filter effects (Ohno, 2002) and first-order Rayleigh scattering. EEMs were collected with a resolution of <2 nm over an excitation range of 250–450 nm and an emission range of 260–800 nm. Nanopure water was used as a blank. The majority of samples (90%) were analyzed with an integration time of 1 s. Lakes with higher fluorescence intensities were analyzed with an integration time of 0.1 s. This is to ensure the accuracy of optical indices as signals exceeding 50,000 counts are outside the linear range of the detector. Fluorescence intensities were scaled for the samples analyzed at 0.1 s. All samples were measured with the high gain setting (2.25 e^{-}/cts) on the CCD detector. Integrated

Raman peak areas for water were obtained from Nanopure water blanks and used to convert the microvolt output of the instrument into Raman units (RU; Lawaetz & Stedmon, 2009).

The fluorescence index (FIX), humification index (HIX), and the index of recent autochthonous contribution (BIX) were calculated using values from the processed EEMs. FIX, the ratio of emission at 450 nm to emission at 500 nm for excitation at 370 nm, can differentiate between microbial and terrestrial sources and is a useful indicator of the aromaticity of the sample. In general, the lower the fluorescence index, the more aromatic the material. The FIX value is about 1.9 for aquatic and microbial sources and about 1.3 for terrestrial and soil sources (Huguet et al., 2009; McKnight et al., 2001). HIX is the ratio of the integrated peak emission intensities from 435 to 480 nm and from 300 to 345 nm at an excitation wavelength of 254 nm. It is an indicator of humification and gives information about the degree of CDOM processing (Chen et al., 2011; Zsolnay et al., 1999). BIX is calculated at an excitation wavelength of 310 nm from the ratio of the emission intensities at 380 and 430 nm. This index corresponds with CDOM production and gives information about recent biological activity (Huguet et al., 2009).

2.6. Absorbance

The Aqualog spectrometer measures absorbance at the same time as fluorescence over the same wavelength range. Napierian absorption coefficients were calculated from absorbance data using Equation 1 (Hu et al., 2002):

$$\alpha = \frac{2.303}{L} \cdot A(\lambda) \tag{1}$$

where $A(\lambda)$ is the measured absorbance at the specified wavelength, α is the Napierian absorption coefficient, and L is the cell path length in meters. Additionally, the specific ultra-violet absorbance (SUVA254) was calculated from the Napierian absorption coefficient at 254 nm and the DOC concentration using Equation 2 (Weishaar et al., 2003).

$$\text{SUVA254} = \frac{\alpha_{254\,nm}}{\text{DOC}} \tag{2}$$

Spectral slopes (S) were calculated by fitting data for S_1 (300–400 nm), S_2 (275–295 nm), and S_3 (350–450 nm) to Equation 3:

$$-S = \frac{\ln\left(\frac{a}{a_0}\right)}{(\lambda - \lambda_0)} \tag{3}$$

α is the absorption coefficient at wavelength λ and α_o is the absorption coefficient at reference wavelength λ_o, which is the highest wavelength in the relevant wavelength range. The slope ratio (S_R) is calculated as the ratio of S_2 to S_3 (Helms et al., 2008).

2.7. Statistical Analyses

The measured EEM spectra were analyzed with parallel factor analysis (PARAFAC) with non-negativity constraints using the *Solo* software package (Eigenvector Research Inc, Washington, USA). PARAFAC analysis makes use of a one-to-one correspondence of the excitation and emission spectra, that is, the emission spectrum is invariant to excitation wavelength and vice versa to decompose EEMs into different component fluorophores. The PARAFAC model was validated using a core consistency diagnostic where the number of modeled components is equal to the largest number of components that maintains a high core consistency (Murphy et al., 2013). The three-component fits used for the measured EEM spectra yielded a core consistency value of 82%. Core consistency figures for two-component, three-component, and four-component fits are shown in Figure S2 in Supporting Information S1. There was a significant decrease in core consistency with the addition of more components (≥4). The residual plots for emission and excitation are given in Figure S3 in Supporting Information S1.

To understand the role of elevation and watershed characteristics on optical properties of lakes, we used a multivariate statistical approach. Specifically, a redundancy analysis (RDA) was appropriate given the range of the data, which was tested with a detrended correspondence analysis (Borcard et al., 2018). Predictor variables included

Table 2
Summary of Water Quality Parameters for Lakes in the Study

Parameter	Minimum	Maximum	Median
Water temperature (°C)	9.9	25.1	22.2
Dissolved oxygen (mg L^{-1})	0.8	12.3	8.9
pH	6.1	9.8	7.9
Specific conductance (μS cm^{-1})	3.3	459.6	78.4
Chlorophyll *a* (μg L^{-1})	0.3	190.3	3.8
Alkalinity (mg L^{-1})	1.2	85.7	26.9
Turbidity (NTU)	0.2	23.5	1.2
Total nitrogen (μg L^{-1})	16.2	2,073.0	397.5
Total phosphorus (μg L^{-1})	5.0	246.8	12.4

Note. Data for individual lakes are provided in Table S3 in Supporting Information S1 (Juetten et al., 2022; https://doi.org/10.25710/6x7v-4858).

landscape variables (elevation, latitude, longitude, surface area, watershed area, and % land use), physico-chemical variables (water temperature, pH, dissolved oxygen, specific conductance, alkalinity, turbidity, TN, and TP), and a biological variable (chlorophyll *a*). Day of year was also included as a covariate to control for differences in sample collection timing. Response variables included DOC, fluorescence (FIX, HIX, and BIX), absorption coefficient at 350 nm (Abs_{350}), SUVA254, and spectral slopes (S_1, S_2, S_3, and S_r). Missing data were estimated using the Bayesian principal component analysis (PCA) method (Oba et al., 2003) in the *pcaMethods* (v. 1.82.0) library in R. This method performs well, particularly when the relative number of missing values is small. In our study, <1% ($n = 14$) values were missing. When predictor variables were highly correlated ($r > |0.75|$), one of the pair was removed from the model. Additionally, predictor variables with a variance inflation factor (VIF) greater than 10, indicating collinearity, were discarded. Forward selection of predictor variables was performed using the approach of Blanchet et al. (2008); only significant predictors were retained in the final model. Analyses were run with the R libraries *vegan* (v. 2.5-7) and *adespatial* (v. 0.3-14).

DOC is a commonly measured variable and integrates processes across both terrestrial and aquatic environments, thus serving as a key indicator of climate change impacts (Adrian et al., 2009). We used a machine learning technique, random forests, to better understand the factors influencing DOC concentrations. Random forests produce a large number of classification trees based on random subsets of predictor and response variables, which are combined to produce accurate predictions, that is, ensemble models. Random forests are largely insensitive to collinearity, can handle nonlinear relationships between response and predictor variables, and can detect interactions between predictor variables (Cutler et al., 2007). Using the *randomForest* (v. 4.6-14; Liaw & Wiener, 2002) and *rfUtilities* (v. 2.1-5; Evans et al., 2011) R libraries, we ran a random forest analysis with $n = 5,000$ trees, with DOC as the response variable and water quality variables as predictors, in addition to landscape variables (elevation, latitude, surface area, watershed area, and % land use). As the presence of other lakes upstream within the watershed could affect DOC concentrations in downstream waters (Goodman et al., 2011), we included a categorical variable to represent whether there was an upstream lake present (1) or not present (0). We excluded variables with high correlations ($r > |0.75|$) to ease model interpretation. We evaluated model performance with pseudo R^2 (% variation explained), mean squared error, and root mean squared error (RMSE; from 10-fold cross-validation). To visualize the marginal effect of each predictor variable (i.e., controlling for other variables), we created partial dependence plots for the top five variables in R library *pdp* (v. 0.7.0; Greenwell, 2017).

3. Results

3.1. Water Quality Data

Detailed water quality data obtained for each lake are given in Table S3 in Supporting Information S1 (Juetten et al., 2022; https://doi.org/10.25710/6x7v-4858), but are summarized here and in Table 2. Dissolved oxygen concentrations largely ranged from 7 to 9 mg L^{-1} (Table 2). Beaver Pond had an unusually low value of 0.8 mg L^{-1}, likely from seasonal anoxia associated with high primary productivity. Surface water temperatures ranged from 9.9 to 25.1°C, reflecting differences in elevation (Figure 2). pH ranged from slightly acidic (6.1) to slightly alkaline (9.8); most lakes were circumneutral (median = 7.8, sd = 0.8). The lakes were all freshwater, with specific conductance values ranging from 3 to 459 μS cm^{-1}; high elevation lakes were typically more dilute (Table 2). Low elevation lakes tended to have higher levels of chlorophyll *a* compared to high elevation lakes (range from 0.3 to 190.3 μg L^{-1}), likely reflecting the lower levels of total nitrogen and total phosphorus in high elevation lakes compared with low elevation lakes (Table 2 and Figure 2).

3.2. DOC Concentrations

DOC concentrations ranged from 0.30 to 16.00 mg L^{-1} across the 62 lakes, with an average of 5.9 ± 3.9 mg L^{-1} (SD) (Table 3). All reported averages in this work are arithmetic means. DOC concentrations in general were

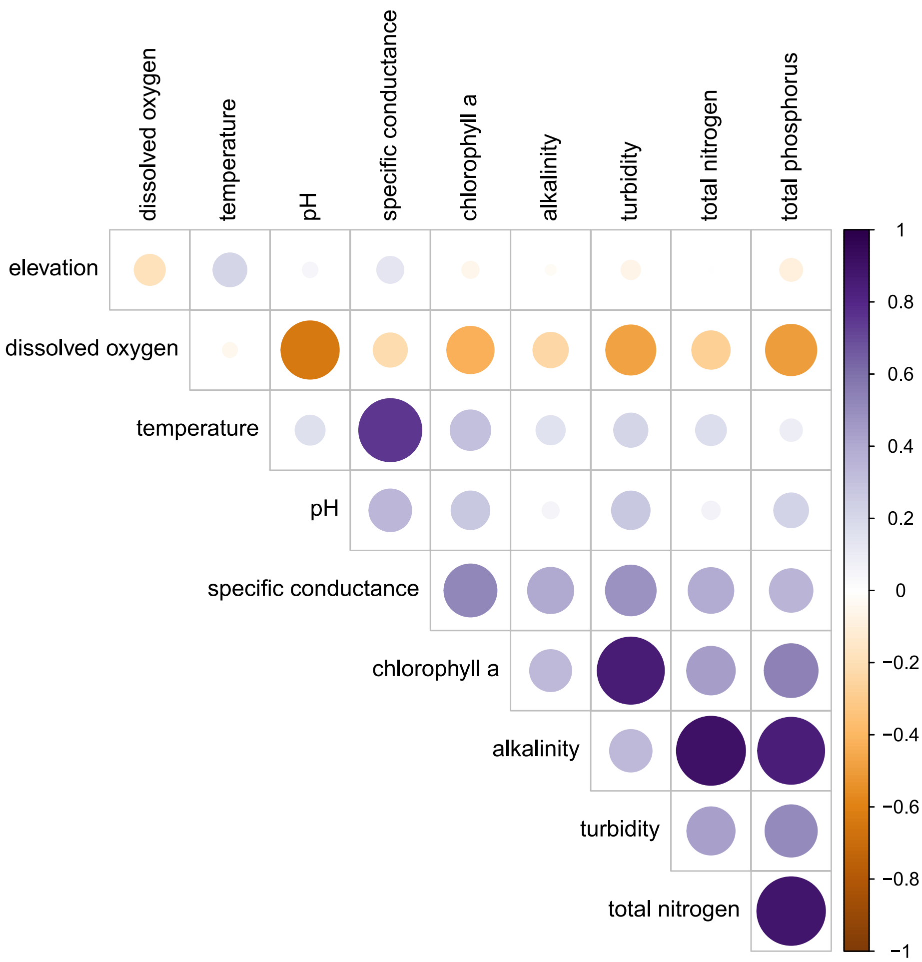

Figure 2. Plot showing Pearson correlation coefficients (r), with positive values in purple and negative values in orange. Darker colors and larger circles represent greater values.

lower for the higher elevation lakes than the lower elevation lakes. Of the lower elevation lakes, Shannon Lake had an unusually low DOC concentration of 0.70 mg L^{-1}, likely owing to the fact that it is a reservoir with a short water residence time, relatively high sedimentation, and is downstream of another reservoir (Baker Lake, not a part of this study).

3.3. Absorbance Measurements

Absorption coefficients are an indicator of the relative amount of CDOM. Absorption coefficients at 350 nm (α_{350}) ranged from 0.06 to 39.97 m^{-1}, with an average of 9.7 ± 9.6 m^{-1} (SD). Absorption coefficients (350 nm) were positively related to DOC concentrations ($R^2 = 0.78$, $p < 0.001$; Figure 3), and were typically lower at higher elevations. Spectral slopes (S) indicate the rate at which CDOM absorption declines with increasing wavelength over various ranges. The spectral slope values in this study ranged from 0.012 to 0.029 nm^{-1}, with an average of 0.017 ± 0.002 nm^{-1} (SD). S_R values ranged from 0.59 to 1.5 (average = 0.99 ± 0.17 (SD)). SUVA254 values ranged from 0.90 to 5.1 mg^{-1} L m^{-1}, with an average of 2.9 ± 1.0 mg^{-1} L m^{-1} (SD).

3.4. Excitation-Emission Matrices

In this study, three fluorescent components were identified (Figure 4). The first component has two peaks with excitation at 250 and 325 nm, respectively, and emission maxima between 450 and 500 nm. This is attributed to terrestrial humic-like material. Component 2 has more blue-shifted emission centered between 375 and

Table 3
Lake DOC Concentrations and Optical Properties, From Low to High Elevation

Lake	Elev	DOC	Abs_{350}	S_1	S_2	S_3	S_R	SUVA254	FIX	HIX	BIX
Cranberry	3	15.4	21.90	0.017	0.017	0.018	0.97	3.0	1.2	4.1	0.8
Lone	6	10.2	13.81	0.018	0.017	0.018	0.94	3.1	1.3	3.1	0.8
Tennant	7	10.7	18.73	0.016	0.014	0.016	0.89	3.0	1.3	4.8	0.7
Honeymoon	8	16.0	39.98	0.016	0.014	0.017	0.85	4.3	1.3	4.1	0.7
Beaver	10	7.1	9.11	0.020	0.017	0.029	0.59	2.9	1.3	3.6	0.7
Clear	11	4.8	5.06	0.018	0.019	0.018	1.10	2.4	1.3	2.9	0.8
Campbell	15	9.9	8.21	0.020	0.021	0.021	1.00	2.5	1.2	3.2	0.8
Wiser	17	11.9	20.66	0.018	0.016	0.019	0.84	3.6	1.2	5.3	0.7
Big	25	3.8	5.83	0.018	0.017	0.018	0.96	3.3	1.2	3.7	0.7
Sunset	32	5.1	4.67	0.019	0.019	0.019	0.99	2.3	1.3	2.6	0.9
Erie	33	12.0	9.58	0.020	0.020	0.019	1.10	2.2	1.3	2.9	0.8
Bug	34	7.4	10.21	0.017	0.016	0.017	0.98	2.8	1.3	3.6	0.8
Hoag	35	10.8	15.41	0.016	0.014	0.016	0.88	2.5	1.3	3.6	0.7
Pass	38	8.0	4.53	0.021	0.023	0.020	1.10	1.8	1.3	2.7	0.8
Fazon	40	12.4	30.27	0.016	0.014	0.016	0.84	4.2	1.2	5.7	0.6
Armstrong	42	5.8	14.57	0.015	0.014	0.015	0.95	4.3	1.1	4.1	0.7
Goss	42	8.2	8.78	0.019	0.019	0.018	1.10	2.8	1.2	3.2	0.8
Ketchum	58	7.7	9.01	0.018	0.018	0.018	0.97	2.7	1.3	3.8	0.8
Martha	58	7.1	8.27	0.019	0.019	0.018	1.00	2.8	1.2	3.5	0.8
Terrell	66	12.3	18.87	0.016	0.015	0.018	0.87	2.7	1.3	4.2	0.8
Sunday	66	8.0	18.34	0.015	0.014	0.014	0.98	3.8	1.2	4.5	0.7
McMurray	69	3.4	3.97	0.019	0.018	0.019	0.96	2.7	1.2	3.4	0.7
Howard	74	5.5	5.04	0.018	0.020	0.017	1.20	2.3	1.2	2.8	0.8
Samish	83	2.5	1.16	0.027	0.023	NA	NA	1.8	1.2	2.2	0.8
Shoecraft	100	4.8	3.45	0.019	0.022	0.018	1.20	2.0	1.2	2.4	0.8
Goodwin	100	4.4	2.10	0.022	0.025	0.020	1.20	1.7	1.3	2	0.9
Heart	103	8.7	4.88	0.020	0.022	0.018	1.20	1.7	1.4	2.5	0.9
Deer	108	5.8	4.42	0.020	0.021	0.020	1.10	2.3	1.3	2.8	0.8
Mirror	111	4.4	12.14	0.015	0.013	0.016	0.82	4.4	1.2	4	0.6
Cain	121	2.8	3.13	0.019	0.019	0.018	1.10	2.7	1.2	3.1	0.7
Reed	122	4.5	10.47	0.016	0.014	0.017	0.81	3.9	1.3	4.2	0.7
Shannon	124	0.7	0.61	0.023	0.021	NA	NA	2.5	1.2	1.5	0.8
Crabapple	126	7.0	10.03	0.018	0.017	0.017	1.00	3.1	1.2	3.6	0.7
Ki	127	3.8	1.15	0.020	0.026	0.018	1.50	1.1	1.2	1.6	0.9
Sixteen	130	5.3	10.13	0.017	0.016	0.017	0.90	3.8	1.2	3.5	0.7
Squires	133	5.6	11.02	0.016	0.014	0.016	0.90	3.4	1.1	3.1	0.7
Whistle	134	7.5	7.36	0.019	0.020	0.019	1.10	2.5	1.2	3.2	0.8
Padden	137	4.8	4.65	0.020	0.019	0.016	1.20	2.6	1.2	2.6	0.7
Squalicum	147	12.0	36.03	0.015	0.013	0.015	0.86	4.9	1.2	6.1	0.6
Geneva	158	10.6	29.40	0.016	0.013	0.016	0.82	4.6	1.2	5.3	0.6
Beaver Pond	158	7.6	21.36	0.015	0.013	0.015	0.87	4.4	1.2	4.2	0.6
Summer	170	7.8	26.31	0.015	0.012	0.015	0.80	5.1	1.1	5.6	0.6
Loma	173	11.0	34.38	0.015	0.013	0.015	0.88	5.0	1.2	5.7	0.6

Table 3
Continued

Lake	Elev	DOC	Abs_{350}	S_1	S_2	S_3	S_R	SUVA254	FIX	HIX	BIX
Everett	201	2.7	5.35	0.016	0.015	0.018	0.84	3.4	1.3	4	0.7
Toad	219	3.1	1.71	0.020	0.022	0.021	1.00	1.6	1.2	3	0.9
Silver	233	1.9	1.90	0.017	0.019	0.019	0.99	2.1	1.2	2	0.8
Grandy	243	2.4	3.45	0.016	0.016	0.017	0.97	2.7	1.3	2.5	0.8
Cavanaugh	308	1.7	1.17	0.019	0.020	0.018	1.10	1.8	1.1	1.8	0.8
Vogler	325	5.6	10.24	0.016	0.015	0.016	0.94	3.3	1.2	3.1	0.6
Monte Cristo	593	1.5	3.59	0.015	0.012	0.017	0.72	3.3	1.3	3.1	0.7
Myrtle	606	5.1	10.29	0.016	0.014	0.015	0.95	3.5	1.1	3.9	0.6
Canyon	708	2.0	4.25	0.017	0.015	0.018	0.84	3.8	1.2	3.6	0.6
Evan	843	4.1	8.05	0.017	0.015	0.017	0.88	3.5	1.1	3.8	0.6
Bear	847	2.2	3.07	0.017	0.017	0.017	0.97	2.8	1.1	3.4	0.6
Coal	1,031	0.6	0.52	0.017	0.020	0.013	1.50	2.1	1.2	0.9	0.8
Highwood	1,253	1.8	3.75	0.016	0.015	0.017	0.87	3.7	1.1	3.3	0.7
Picture	1,255	2.2	3.42	0.018	0.017	0.021	0.82	3.2	1.1	3	0.7
L. Bagley	1,276	0.3	0.75	0.012	0.014	0.010	1.35	3.4	1.1	1.1	0.6
Sunrise	1,292	2.2	2.35	0.019	0.019	0.020	0.95	2.5	1.2	2	0.9
U. Bagley	1,321	0.3	0.44	0.014	0.016	0.013	1.18	2.5	1.2	1	0.8
U. Twin	1,574	0.4	0.12	NA	0.024	NA	NA	1.2	1.2	0.6	0.8
L. Twin	1,574	0.5	0.06	NA	0.029	NA	NA	0.9	0.2	1	1.1

Note. Elevation (m), dissolved organic carbon (DOC; mg L^{-1}), absorption coefficient (Abs_{350}; m^{-1}), spectral slopes (S_x; nm^{-1}), specific ultra-violet absorbance (SUVA254; mg^{-1} L m^{-1}), fluorescence index (FIX; unitless), humification index (HIX; unitless), and the index of recent autochthonous contribution (BIX; unitless). Location information for each lake is given in Supporting Information S1.

425 nm; this is attributed to microbially altered terrestrial humic-like material. Component 3 has one peak with an excitation at 375 nm and emission between 300 and 350 nm; this is attributed to protein-like organic matter.

The humic components were found in all but two lakes in this study. The exceptions were Coal Lake and Upper Twin Lake, which are both high elevation systems. The intensities of the humic components ranged from 3.78 to 14.31 RU; fluorescence intensities were generally lower at higher elevations. Component 3 is typically associated with the amino acid tryptophan and is often referred to in the literature as a protein-like peak (Osburn et al., 2011). The protein-like component 3 was observed in 40 of the 62 sample lakes. The intensity ranged from 1.14 to 8.4 RU with higher intensities in the lower elevation lakes and an average that was lower than the average intensity for the humic components. However, the intensity of the protein component was higher than that for the humic components for five out of eight lakes above 1,000 m.

The relative abundance of component 1 varies from 12% to 63%, with most lakes having component 1 as 40%–60% of the overall pool. Component 2 had a lower relative abundance, ranging from 14% to 46%, with most lakes in the range of 30%–40%. Component 3 ranged from 1% to 70%, with most lakes below 30%. The relative abundance of component 3, the protein-like component, is generally lower for the low elevation lakes and increases with increasing elevation, forming the major component in the highest elevation lakes (Figure 5). The relative proportion of components 1 and 2, the terrestrial humic material, decreased with increasing elevation, as the proportion of the protein component increased.

3.5. Fluorescence Indices

The fluorescence indices are given in Table 3. BIX values varied from 0.6 to 0.9 with an average of 0.74 ± 0.10 (SD) and FIX values ranged from 1.1 to 1.4 with an average of 1.2 ± 0.15 (SD). Lower Twin Lake, a high elevation lake that had unusual SUVA254 and absorption coefficient values, also had an unusually low FIX value of

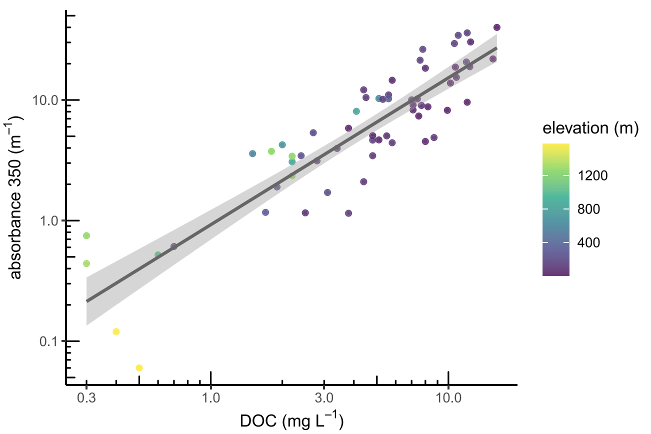

Figure 3. The relationship between dissolved organic carbon (DOC) concentration (in mg L^{-1}) and absorption coefficient α_{350} (in m^{-1}) across lakes, with symbol color representing lake elevation (m) ($n = 62$). Data are plotted on a $\log_{10}$ scale. Regression line (±95% confidence interval): $y = 1.218 * x - 0.034$.

0.2 and an unusually high BIX value of 1.1. The BIX and FIX values for Lower Twin Lake are excluded from the above ranges. Values for the humification index HIX ranged from 0.6 to 6.1, with an average value of 3.3 ± 1.2 (SD). HIX values were typically higher for lower elevation lakes.

3.6. Relationships Between DOC and CDOM Properties and Landscape Variables and Water Quality Parameters

We used a redundancy analysis (RDA) to explore relationships between CDOM optical properties and water quality variables and lake and watershed characteristics (Figure 6). Including all significant variables, RDA axes 1 and 2 explained 41.5% of variance (adjusted R^2) in CDOM variables and the overall RDA was significant ($F = 8.82$, $p < 0.001$, $n = 999$ permutations). Significant predictor variables included elevation, pH, chlorophyll *a*, surface area, and watershed area (all $p < 0.05$). The first axis separates lakes with large watershed area and high SUVA254, absorption coefficient at 350 nm (Abs350), and humification index (HIX) values from lakes with large lake surface areas, high spectral slopes (S_2 and S_r) and, to a lesser degree, BIX (~CDOM production, representing recent biological activity). The second axis contrasts high elevation lakes from those with high pH, chlorophyll a, DOC, S_3, and the fluorescence index (FIX). Lakes with large surface areas were positively correlated with spectral slopes (S_1, S_2, and S_r) and BIX, and negatively correlated with SUVA254. Lake surface area was not correlated with elevation, DOC, or absorption coefficient at 350 nm.

Correlations between CDOM optical properties were observed (Figure 6). For example, *S* values were negatively correlated with SUVA254 values, as would be expected since lower *S* and higher SUVA254 are both associated with increased aromaticity. BIX values, an indicator for more allochthonous material inputs, were positively correlated with spectral slopes and negatively correlated with SUVA254, indicators of increased aromaticity. HIX values are negatively correlated with S_R, indicating reduced amounts of humic material with an index that indicates autochthonous production.

3.7. Modeling Controls on DOC in Lakes

We examined the factors influencing DOC as a key indicator variable in lakes with a random forest analysis. The observed positive correlation between absorbance and DOC (Figures 3 and 6) suggests that DOC and CDOM are related and therefore that the factors that influence DOC concentrations likely also influence the amount of CDOM. The model explained ~77% of variance in DOC and had low overall error rates (pseudo $R^2 = 76.7\%$, mean squared error = 3.53, root mean squared error from cross-validation = 0.33). The variables that explained the most variation in DOC included total nitrogen (TN) and total phosphorus (TP), followed by a group of variables with similar importance, including elevation, day of year, water temperature, % agriculture, and specific conductance (Figure 7a). Partial dependence plots provide more insight on these relationships, controlling for the confounding effects of other covariates (Figures 7b–7k). These plots suggest that variables like TN, TP, specific conductance, % agriculture, and % wetland have a positive effect on DOC up to a threshold, after which no more increases are observed. Conversely, water temperature only had a positive effect on DOC at higher temperatures (Figure 7f). Finally, elevation, day of year, latitude, and dissolved oxygen had nonlinear relationships with DOC. DOC declined steeply with elevation up to ~250 m, but at elevations >250 m, only slight changes in DOC were observed (Figure 7d). Conversely, day of year had modest positive effects on DOC until ~ day 220 (early August), after which negative effects were observed (Figure 7e). This latter result may be an artifact of sampling, where higher elevation lakes tended to be sampled later in the summer after ice-off. DOC was constant at low values of latitude and dissolved oxygen, then decreased at moderate values (48.0–48.6 and 7.5–10.0 mg L^{-1}, respectively), at which point slight increases were observed at the highest values (Figures 7j and 7k).

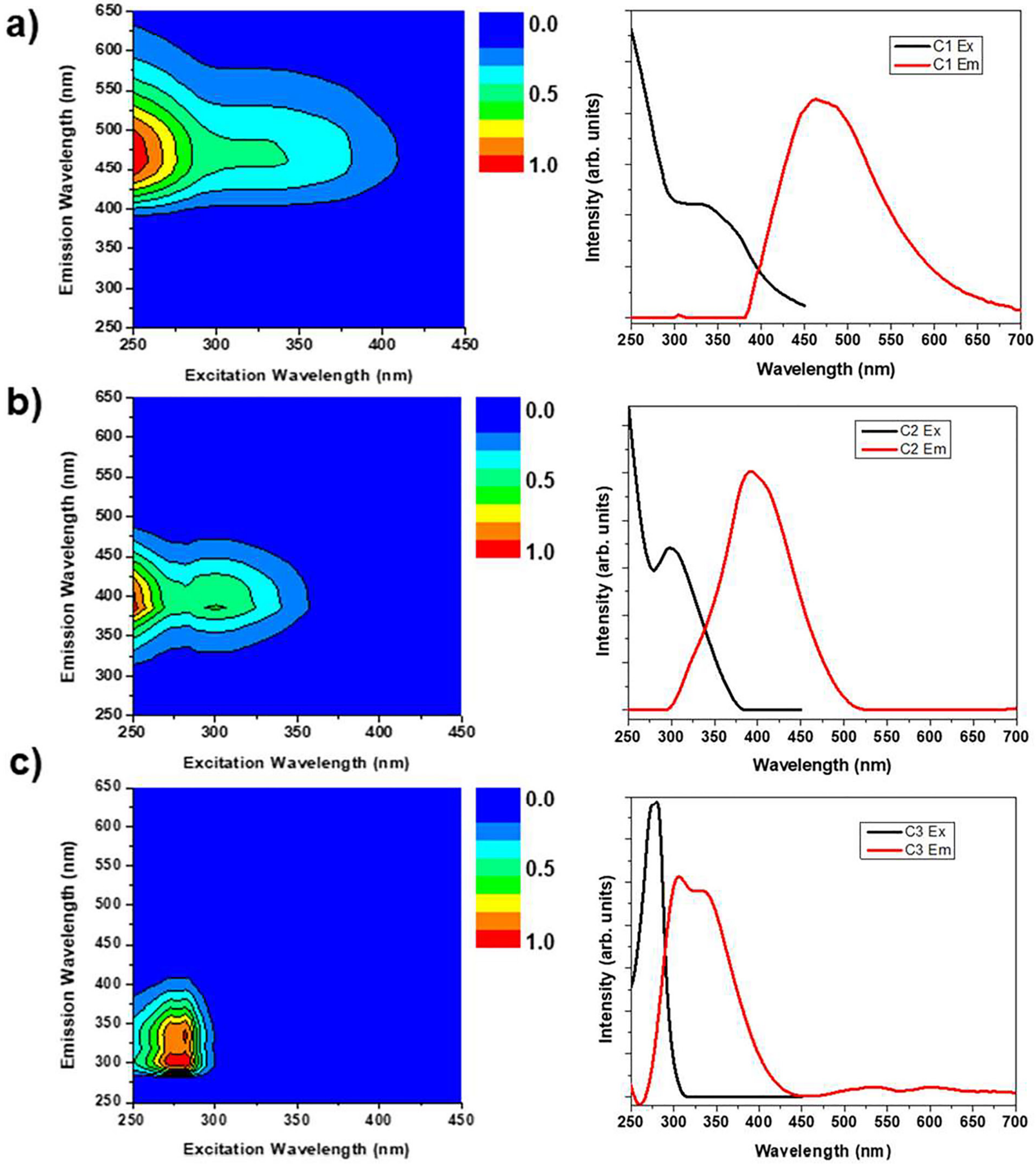

Figure 4. Three fluorescent components identified by PARAFAC analysis: (a) component 1: terrestrial humic-like; (b) component 2: microbially altered terrestrial humic-like; (c) component 3: protein-like organic matter. The intensity scale is from the PARAFAC fitting and is normalized to a maximum of 1.

4. Discussion

4.1. Variations in DOC Concentrations and Land Use Characteristics With Elevation

The DOC concentrations ranging from 0.30 to 16.00 mg L^{-1} (median 5.20 mg L^{-1}) measured here are consistent with prior lake studies (see, e.g., Laurion et al., 2000; Rantala et al., 2016; Song, Li, et al., 2019; Song, Shang, et al., 2019). The range of values fall within levels found for lake ecosystems in a review of 7,500 lake measurements across six continents (median of 5.71 mg/L; Sobek et al., 2007). Variations in DOC concentrations between

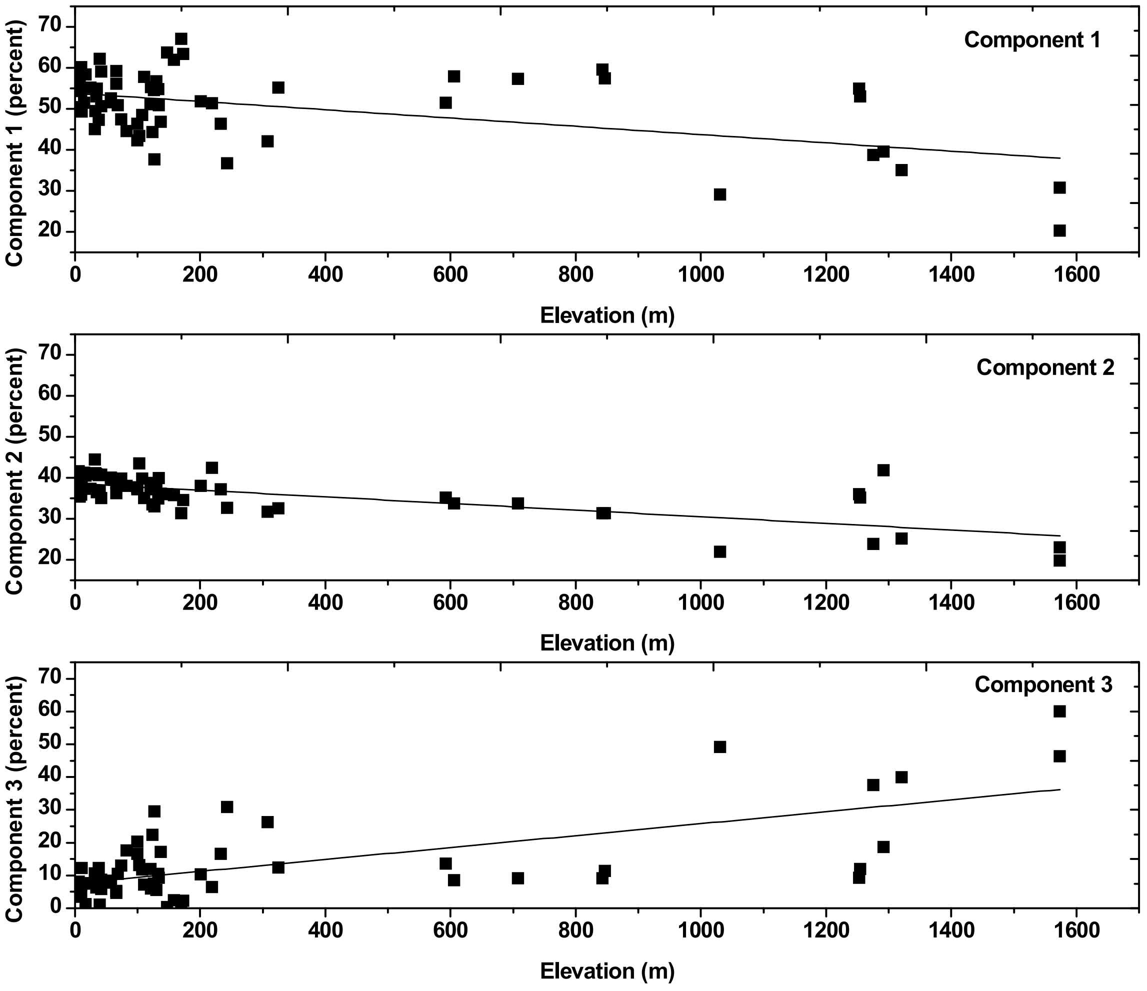

Figure 5. Relative percentage of components 1, 2, and 3 as a function of elevation. R^2 for component 1 = 0.251; component 2 = 0.494; component 3 = 0.447. $n = 62$ and $p < 0.001$ for all three components.

different elevation lakes have been attributed to regional climate and topographic characteristics together with specific watershed and lake properties (Sobek et al., 2007). Additional correlations were found between DOC and precipitation, mean annual runoff, conductivity, and soil carbon density (Sobek et al., 2007).

DOC concentrations were lower in higher elevation lakes in our study. Higher elevation lakes tended to have lower water temperatures, low nutrients and low chlorophyll *a*. Lakes here did not extend above the treeline, though % forest cover was lower at the highest elevation lakes compared to more intermediate elevations: % forest cover showed a unimodal relationship with elevation, with no significant correlation ($\rho = -0.14$, $p = 0.26$) (Figure S5 in Supporting Information S1). The total amount of vegetation coverage increased with elevation ($\rho = 0.26$, $p = 0.04$), while the type of vegetation coverage changed. For example, the relative amount of wetlands and agriculture in the watershed decreased with elevation (% wetland: $\rho = -0.56$, $p < 0.001$; % agriculture: $\rho = -0.70$, $p < 0.001$), while the relative amount of herbaceous shrubs increased, though not significantly ($\rho = 0.24$, $p = 0.062$) (Figure S5 in Supporting Information S1).

DOC levels in this study were positively influenced by total nitrogen and total phosphorous (Figure 7), as well as chlorophyll *a* (Figure 6). This is consistent with the quantity of DOC in the lakes depending primarily on runoff from the watershed. Zhang et al. (2010) attributed increasing total nitrogen, total phosphorous, and chlorophyll *a* concentrations in lower elevation lakes to increased anthropogenic and terrestrial inputs caused by human activity in the watershed. However, DOC concentrations were not related to lake surface area or watershed area. This suggests that higher DOC concentrations at lower elevations are primarily driven by increased terrestrial inputs associated with different types of vegetation coverage and land use. DOC was positively influ-

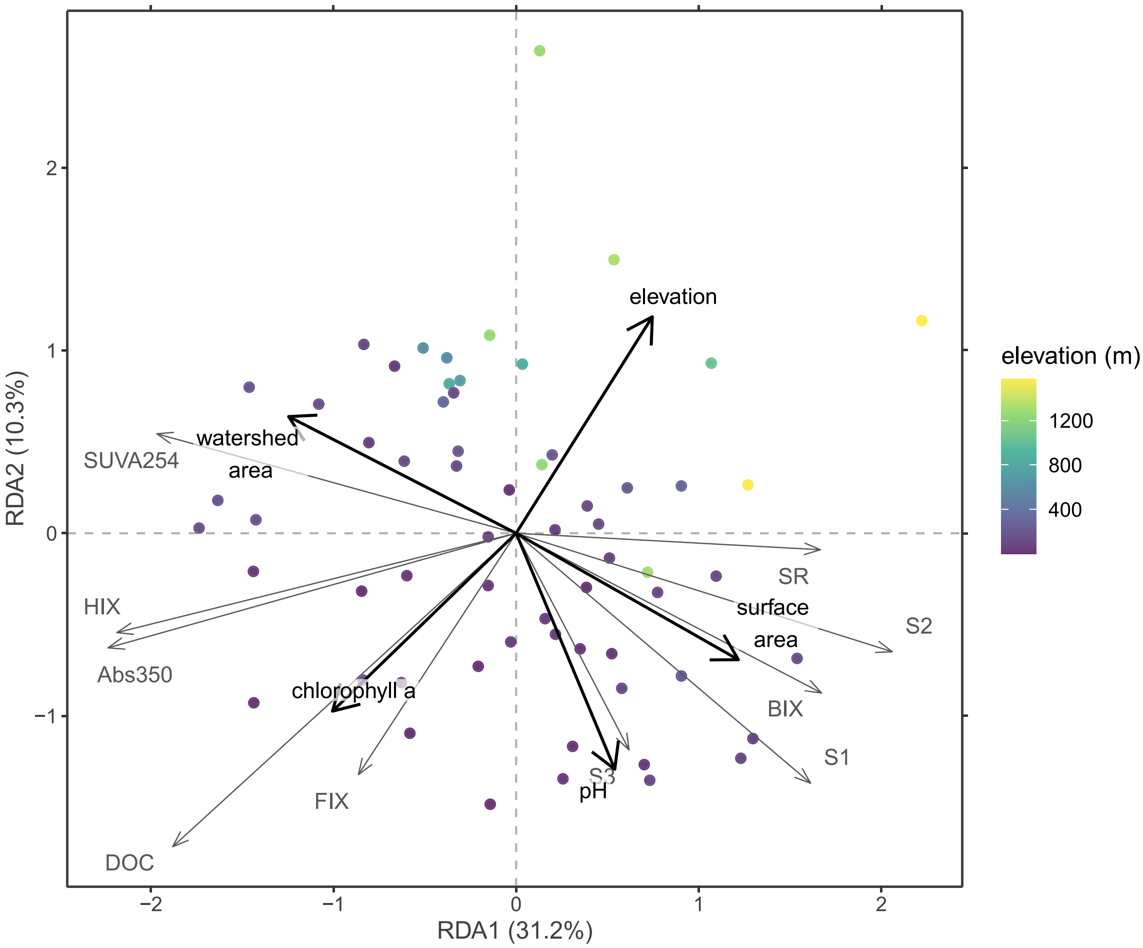

Figure 6. Redundancy analysis plot, where black arrows indicate significant environmental predictors, gray arrows represent chromophoric dissolved organic matter properties (response variables), and circles represent lakes, colored from low elevation (purple) to high elevation (yellow). Abbreviations described in text. Lake names are shown in Figure S4 in Supporting Information S1 (Juetten et al., 2022; https://doi.org/10.25710/6x7v-4858). In general, the angles between the variables represent correlations, where small angles are positive correlations, large angles are negative correlations, and right angles are uncorrelated. For example, chlorophyll *a* is positively correlated with dissolved organic carbon (and other variables in close proximity), whereas chlorophyll *a* is negatively correlated with elevation.

enced by % agriculture and % wetlands (Figure 7), which were generally higher at lower elevations (Figure S5 in Supporting Information S1). In prior studies on high elevation alpine and sub-alpine lakes (Winn et al., 2009) and the temperate Great Lakes (Xenopoulos et al., 2003), DOC concentrations were positively correlated with wetland coverage in the watershed. Wetland cover was also identified as the primary driver of the aquatic carbon pool in a study on subarctic Finnish lakes (Rantala et al., 2016). Increased biological production driven by higher nutrient inflow could also be important in low elevation lakes. This is consistent with the higher levels of the protein-like fluorescent component 3 observed at lower elevations. DOC also had a moderate positive relationship with specific conductance (Figure 7), which may be due to concentration by evaporation (Osburn et al., 2011) or more likely erosion material entering the streams in the watershed.

4.2. Variations in CDOM With Elevation

CDOM represents the fraction of the DOM pool (of which DOC is a measure) that absorbs sunlight. Variability in CDOM optical properties can be attributed to, and provide information about, the amount of organic material as well as the source and processing of that material. Absorption coefficient and fluorescence generally change as the amount of CDOM changes, whereas spectral slopes, fluorescence indices, and spectral slope ratios change as organic material is processed and/or as the source of the material changes (Bowen et al., 2017; Boyd & Obsurn, 2004; Clark et al., 2014, 2020; Del Vecchio & Blough, 2004; Green & Blough, 1994; Helms et al., 2008).

10.1029/2022EA002503

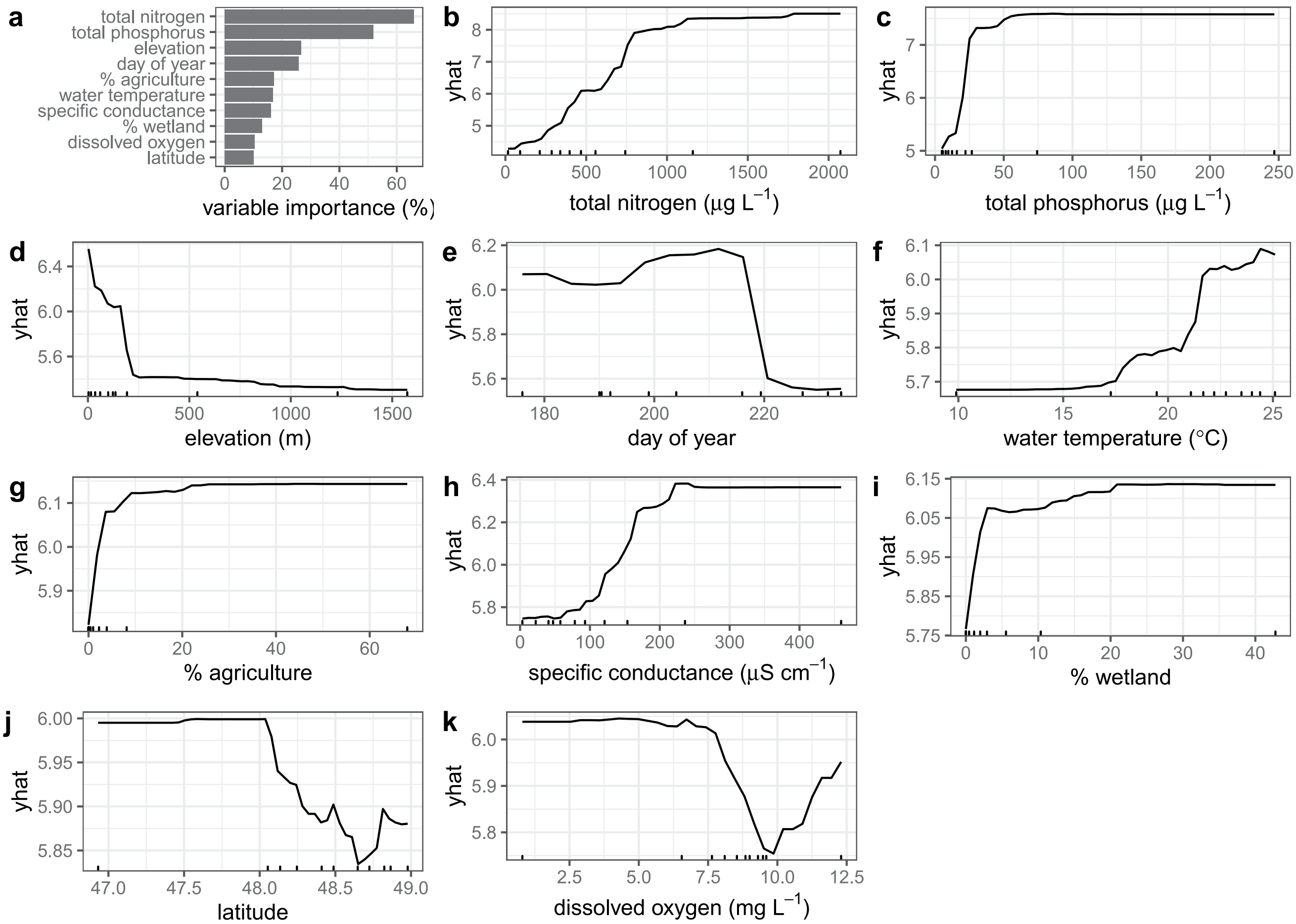

Figure 7. (a) Variable importance plot for random forest analysis (showing the top 10 variables), followed by partial dependence plots for (b) total nitrogen (μg L^{-1}), (c) total phosphorus (μg L^{-1}), (d) elevation (m), (e) day of year, (f) water temperature, (g) % agriculture, (h) specific conductance (μS cm^{-1}), (i) % wetland, (j) latitude, and (k) dissolved oxygen (mg L^{-1}). The *y*-axes are unitless, representing the marginal effect of the predictor variable on dissolved organic carbon (i.e., yhat). Vertical black lines within the plot on the *x*-axes represent the deciles of the observed values of each predictor.

CDOM in lakes has been attributed to a mixture of allochthonous terrestrial material from the watershed and autochthonous material produced in situ by biota (Zhang et al., 2010). Autochthonous production includes extracellular release by phytoplankton, release by grazers, and lysis of plankton (Tranvik et al., 2009). Levels are controlled by the physical and chemical properties of the lake and nutrient availability. Allochthonous inputs are a result of terrestrial runoff and, similar to DOC, are often controlled by the size of the watershed area, amount of vegetation coverage, and vegetation type. Both allochthonous and autochthonous materials are impacted by biological and photochemical processing. However, allochthonous DOM is more susceptible to photochemical and biological processing than autochthonous material (Catalan et al., 2013). We would expect higher UV exposure for lakes at higher elevations and thus increased photochemical processing. More biological processing might be expected in lower elevation lakes with higher nutrient and chlorophyll levels. These relationships are often confounded by a suite of physical and chemical properties of lake water that impact absorbance and fluorescence directly. For example, pH, metal ion concentrations, and buffering capacity have been shown to affect some optical properties like fluorescence intensity and fluorescent peak locations (Baker et al., 2008; Patel-Sorrentino et al., 2002; Yamashita & Jaffe, 2008). Trends in optical properties with elevation associated with changes in the amount, sources, and processing of CDOM are discussed in the next three sections.

4.2.1. Variations in Optical Properties Associated With the Quantity of CDOM With Elevation

Absorption coefficients measured here are consistent with prior studies (e.g., Osburn et al., 2011; Yao et al., 2011; Zhang, Yin, Liu, et al., 2011). The positive relationship between the absorption coefficient and DOC (Figure 3) suggests an underlying relationship between CDOM (i.e., absorption coefficients) and a measure of the DOM pool (i.e., DOC concentrations). This has been reported in the literature (e.g., Aulio-Maestro et al., 2017; DeVilbiss et al., 2016; Xu et al., 2017; Ylostalo et al., 2014; Zhang et al., 2007). Absorption coefficients (350 nm) and fluorescence intensities were lower in higher elevation lakes (Figure 6). Given the similar trend in DOC, the simplest explanation is that there are higher amounts of CDOM at lower elevations. However, absorption coefficients can be influenced as CDOM is photochemically or biologically processed and fluorescence can be affected by the physio-chemical properties of the water. For example, Patel-Sorrentino et al. (2002) saw an increase of humic-like fluorescence intensities with pH in rivers. However, humic-like fluorescent component intensities were not correlated with pH in our work, suggesting that changes in fluorescence are associated with changes in the amount of fluorescent material. Similarly, one might expect more photobleaching in the higher elevation lakes or more biological processing in the lower elevation lakes, which could influence trends in the absorption coefficient with elevation. However, optical parameters like the spectral slopes, which give an indication of the degree of processing, did not vary with elevation (Figure 6; discussed further below). This suggests that photobleaching or biological processing is not the dominant driver of absorption coefficient changes with elevation. Lower absorption coefficients with higher elevation are therefore likely the result of decreases in the amount of CDOM.

As with DOC, decreases in the absorption coefficient with elevation are not unexpected when the elevation range extends above the treeline and the overall amount of vegetation coverage decreases. For example, Olson et al. (2018) observed an increase in CDOM absorbance with the percentage of the catchment covered by vegetation in a study on mountain lakes where several of the lakes were above the treeline and had little to no vegetation cover. Overall vegetation coverage in watersheds in our study increased with elevation, while vegetation type changed. The watersheds of the higher elevation lakes had no agriculture or wetland vegetation and tended to be dominated by herbaceous-shrub vegetation instead of forested cover (Figure S5 in Supporting Information S1). In our study, absorption coefficients were positively correlated with % wetlands ($r = 0.42$, $p < 0.001$) and moderately positively correlated with % agriculture ($r = 0.25$, $p = 0.049$), but not with other land cover classes. This suggests that the dominant drivers of CDOM inputs in this region are wetlands and agriculture. Overall, the land cover characteristics of watersheds play an important role in controlling CDOM input to lakes.

4.2.2. Trends in Indicators of CDOM Sources With Elevation

In this study, three fluorescent components were identified from the PARAFAC analysis of the lake EEMs. Components similar to component 1 in this study have been attributed to terrestrial humic-like material (Du et al., 2016; Kothawala et al., 2012; Stedmon et al., 2003; Tank et al., 2011; Xiao et al., 2019). Components similar to component 2 in our study have been attributed to microbially-derived humic material or phytoplankton degradation products (Kim et al., 2022; Zhang et al., 2010; Zhang, Yin, Liu, et al., 2011). We attribute component 2 to terrestrial humic material that has undergone microbial processing, as identified in Zhou et al. (2016) in the Great Lakes. A component similar to component 3 has been attributed to protein-like material (see, e.g., Tank et al., 2011; Zhang, Yin, Feng, et al., 2011).

In our work, the fluorescence of both the humic-like and protein-like components decreased with increasing elevation, consistent with trends in DOC and absorbance. However, the ratio of the protein-like to humic-like fluorescence intensity increased with elevation. The most prevalent and intense components across all but five of the lakes were the humic-like components. This is consistent with the CDOM pool being dominated by terrestrial runoff for most lakes. The protein-like component is an indicator of autochthonous production from microbial sources (Hayakawa et al., 2016). This increased at lower elevations, consistent with increased biological production in lakes with higher nutrient levels. The lakes for which the protein-like component was dominant rather than the humic-like components were high elevation lakes; five out of 8 lakes above 1,000 m had a more intense protein-like component. This may be due to a limited terrestrial source for these lakes, or a burst of autochthonous production following ice-off/spring-summer runoff. Two of the lakes above 1,000 m had no detectable humic-like components (Coal and Upper Twin).

Trends and values of SUVA254 and S_R, potential indicators of source, are consistent with the observed trends in the humic-like and protein-like components. SUVA254 gives an indication of the degree of aromaticity. Higher SUVA254 values are associated with increased aromaticity and allochthonous terrestrial material (Weishar et al., 2003). Similar values to the range of 0.90–5.1 mg^{-1} L m^{-1} (average 2.9 ± 1.0 mg^{-1} L m^{-1} SD) measured here have been reported in prior studies (Griffin et al., 2018; Song, Li, et al., 2019; Song, Shang, et al., 2019). SUVA254 was positively correlated with the absorption coefficient ($r = 0.74$, $p < 0.001$; Figure 6), indicating more aromatic material associated with higher levels of CDOM. This is consistent with increased inputs of more aromatic terrestrial material at lower elevations (McKnight & Aiken, 1998; McKnight et al., 2001). S_R values > 1 are attributed to autochthonous material, and S_R values < 1 are attributed to terrestrial material (Zhang, Yin, Liu, et al., 2011). S_R was negatively correlated with the absorption coefficient ($r = -0.48$, $p < 0.001$), indicating more allochthonous material at lower elevations where CDOM inputs are higher. The majority of lakes had S_R values < 1 (71%), corresponding to a dominant terrestrial source. Three of the five lakes above 1,000 m with the more intense protein-like component had S_R values > 1 (two were not calculated due to issues fitting spectral slopes for those samples).

The fluorescent indices are consistent with trends observed in the PARAFAC components. HIX values are an indication of the degree of humification. Higher values are associated with more humic, terrestrial material. High elevation lakes had HIX values <1.1, consistent with less humic material. Low elevation lakes had higher absorption coefficients and higher HIX values, consistent with increased allochthonous inputs of more humic material. BIX values <0.6 are associated with terrestrial inputs and values >1 are attributed to autochthonous sources (Weiwei et al., 2018; Zhou et al., 2016). BIX values ranged from 0.6 to 1.1, with an average of 0.74 ± 0.10 (SD). Lower Twin Lake, the highest elevation lake, is the only lake with a BIX value >1. About half of the lakes had BIX values between 0.6 and 0.7, suggesting that terrestrial material dominates. FlX values around 1.3 indicate terrestrial material and values >1.9 indicate aquatic microbial sources (Huguet et al., 2009; McKnight et al., 2001). FlX values measured here (~1.1–1.2) are consistent with a dominant terrestrial allochthonous source.

These fluorescent results and optical indices indicate increased amounts of more humic material at lower elevation and increased contributions from protein-like material at higher elevations. Two possible explanations for this trend are that allochthonous terrestrial material is reduced at elevation relative to in situ production of autochthonous material due to different vegetation types, or that photochemical degradation is increased for allochthonous terrestrial material versus autochthonous material in higher elevation lakes.

4.2.3. Trends in Indicators of CDOM Processing With Elevation

While it can be difficult to compare S values when different wavelength ranges are used to calculate the spectral slope, overall values obtained here are consistent with the literature (Aulio-Maestro et al., 2017; Ylostalo et al., 2014; Zhang & Qin, 2007). Changes in spectral slopes may be associated with changes in CDOM structure due to processing. Increases in S have been attributed to photochemical and biological processing, and decreasing molecular weight (Osburn et al., 2011). Different values at elevation might be expected based on increased levels of solar radiation and hence increased photobleaching degrading the more aromatic allochthonous portion of the DOM pool more rapidly (Catalan et al., 2013). S values were independent of elevation in an earlier study on mountain lakes (Laurion et al., 2000), but increased at higher elevations above the treeline in another study (Su et al., 2015). No significant correlations between S values and elevation were observed in our study (Figure 6). This suggests that increased inputs of autochthonous material and photobleaching are not sufficient to alter some of the optical characteristics of CDOM from terrestrial sources in high elevation lakes. Rainfall and snow melt over the summer months contribute terrestrial CDOM to the highest elevation lakes, potentially offsetting optical signals associated with processing of the more aged CDOM already in situ.

5. Conclusions

Optical parameters for lakes in the Pacific Northwest indicate they are largely dominated by allochthonous terrestrial sources of CDOM from the watershed. The optical parameters associated with CDOM quantity showed significant differences with elevation. There are lower levels of CDOM in higher elevation lakes based on lower DOC concentrations, absorption coefficients at 350 nm and fluorescence intensities. This is attributed to reduced inputs from different vegetation types. Higher elevation lakes had a relatively high amount of herbaceous-shrub vegetation in their watersheds (% cover), compared to greater forest cover at more intermediate elevations and higher amounts of wetland and agriculture cover at lower elevations. Some of the optical parameters associated with CDOM source and processing also showed elevational differences. Specifically, increases in the relative contribution of protein-like organic matter fluorescence and lower HIX values at higher elevations are consistent with a greater relative contribution from autochthonous CDOM. This may be due to decreased inputs of allochthonous humic material caused by shifts in types of vegetation for the high elevation lakes, or to increased photochemical and biological processing of terrestrial allochthonous material compared to autochthonous material produced in situ from microorganisms. We observed that some water quality variables exhibited nonlinear dynamics with DOC, suggestive of thresholds related to a suite of characteristics in lakes and watersheds that change with elevation. For example, DOC concentration increased with % wetland cover in watersheds until it reached a threshold around 5% (i.e., wetlands made up 5% of watershed land cover), after which effects of wetlands on DOC were marginal. These results underline the complexity of processes involved in the accumulation, formation, and photochemical and biological processing of dissolved organic matter. Given expected shifts in tree cover from climate change, particularly at higher elevations, DOC and other CDOM properties of lakes will likely change in the future.

Data Availability Statement

The supporting data used in this study are available in CEDAR, the online repository of Western Washington University (Juetten et al., 2022; https://doi.org/10.25710/6x7v-4858).

Acknowledgments
The authors thank the Institute for Watershed Studies: Michael Hilles for the DOC measurements, Joan Pickens for coordinating lake sampling, Garrett McHugh and Aurora Watts for collecting samples, and Robin Matthews for study design and support. The authors thank the reviewers for their helpful comments and input.

References

Adrian, R., O'Reilly, C. M., Zagarese, H., Baines, S. B., Hessen, D. O., Keller, W., et al. (2009). Lakes as sentinels of climate change. *Limnology & Oceanography*, *54*(6part2), 2283–2297. https://doi.org/10.4319/lo.2009.54.6_part_2.2283

Allesson, L., Koehler, B., Thrane, J.-E., Andersen, T., & Hessen, D. O. (2021). The role of photomineralization for CO_2 emissions in boreal lakes along a gradient of dissolved organic matter. *Limnology & Oceanography*, *66*(1), 158–170. https://doi.org/10.1002/lno.11594

APHA. (1989). *Standard methods for the examination of water and wastewater* (17th ed.). American Public Health Association.

Arvola, L., Aijala, C., & Lepparanta, M. (2016). CDOM concentrations of large Finnish lakes relative to their landscape properties. *Hydrobiology*, *780*(1), 37–46. https://doi.org/10.1007/s10750-016-2906-4

Aulio-maestro, M., Hunter, P., Spyrakos, E., Mercatoris, P., Kovacs, A., Horvath, H., et al. (2017). Spatio-seasonal variability of chromophoric dissolved organic matter absorption responses to photobleaching in a large shallow temperate lake. *Biogeo*, *14*, 1215–1233.

Baker, A., Tipping, E., Thacker, S. A., & Gondar, D. (2008). Relating dissolved organic matter fluorescence and functional properties. *Chemosphere*, *73*(11), 1765–1772. https://doi.org/10.1016/j.chemosphere.2008.09.018

Blanchet, F. G., Legendre, P., & Borcard., D. (2008). Forward selection of explanatory variables. *Ecology*, *89*, 2623–2632.

Borcard, D., Gillet, F., & Legendre, P. (2018). *Numerical ecology with R* (2nd ed., p. 435). Springer.

Bowen, J. C., Clark, C. D., Keller, J. K., & De Bruyn, W. J. (2017). Optical properties of chromophoric dissolved organic matter (CDOM) in surface and pore waters adjacent to an oil well in a southern California salt marsh. *Marine Pollution Bulletin*, *114*(1), 157–168. https://doi.org/10.1016/j.marpolbul.2016.08.071

Boyd, T. J., & Obsurn, C. L. (2004). Changes in CDOM fluorescence from allochthonous and autochthonous sources during tidal mixing and bacterial degradation in two coastal estuaries. *Marine Chemistry*, *89*(1–4), 189–210. https://doi.org/10.1016/j.marchem.2004.02.012

Catalan, N., Obrador, B., Felip, M., & Pretus, J. L. (2013). Higher reactivity of allochthonous vs. autochthonous DOC sources in a shallow lake. *Aquatic Sciences*, *75*(4), 581–593. https://doi.org/10.1007/s00027-013-0302-y

Chen, H., Zheng, B., Song, Y., & Qin, Y. (2011). Correlation between molecular absorption spectral slope ratios and fluorescence humification indices in characterizing CDOM. *Aquatic Sciences*, *73*(1), 103–112. https://doi.org/10.1007/s00027-010-0164-5

Clark, C. D., Aiona, P., Keller, J. K., & De Bruyn, W. J. (2014). Optical characterization and distribution of chromophoric dissolved organic matter (CDOM) in soil porewater from a salt marsh ecosystem. *Marine Ecology Progress Series*, *516*, 71–83. https://doi.org/10.3354/meps10833

Clark, C. D., De Bruyn, W. J., Brahm, B., & Aiona, P. (2020). Optical properties of chromophoric dissolved organic matter (CDOM) and dissolved organic carbon (DOC) levels in constructed water treatment wetlands in Southern California, USA. *Chemosphere*, *247*, 125906. https://doi.org/10.1016/j.chemosphere.2020.125906

Creed, I. F., Bergström, A.-K., Trick, C. G., Grimm, N. B., Hessen, D. O., Karlsson, J., et al. (2018). Global change-driven effects on dissolved organic matter composition: Implications for food webs of northern lakes. *Global Change Biology*, *24*(8), 3692–3714. https://doi.org/10.1111/gcb.14129

Cutler, D. R., Edwards, T. C., Jr., Beard, K. H., Cutler, A., Hess, K. T., Gibson, J., & Lawler, J. J. (2007). Random forests for classification in ecology. *Ecology*, *88*(11), 2783–2792. https://doi.org/10.1890/07-0539.1

De Laurentiis, E., Minella, M., Maurino, V., Minero, C., Brigante, M., Mailhot, G., & Vione, D. (2012). Photochemical production of organic matter triplet states in water samples from mountain lakes, located below or above the tree line. *Chemosphere*, *88*(10), 1208–1213. https://doi.org/10.1016/j.chemosphere.2012.03.071

De Vilbiss, S. E., Zhou, Z., Val Klump, J., & Guo, L. (2016). Spatiotemporal variations in the abundance and composition of bulk and chromophoric dissolved organic matter in seasonally hypoxia-influenced Green Bay, Lake Michigan, USA. *Science of the Total Environment*, *565*, 742–757.

Del Vecchio, R., & Blough, N. V. (2004). On the origin of the optical properties of humic substances. *Environmental Science & Technology*, *38*(14), 3885–3891. https://doi.org/10.1021/es049912h

Dewitz, J., & U.S. Geological Survey. (2021). *National Land Cover Database (NLCD) 2019 products (v 2.0, June 2021)*. U.S. Geological Survey data release. https://doi.org/10.5066/P9KZCM54

Du, Y., Zhang, Y., Chen, F., Chang, Y., & Liu, Z. (2016). Photochemical reactivities of dissolved organic matter (DOM) in a sub-alpine lake revealed by PARAFAC: And insight into the fate of allochthonous DOM in alpine lakes affected by climate change. *Science of the Total Environment*, *568*, 216–225. https://doi.org/10.1016/j.scitotenv.2016.06.036

Eklof, K., von Bromssen, C., Amvrosiadi, N., Folsteer, J., Wallin, M. B., & Bishop, K. (2021). Brownification on hold: What traditional analyses miss in extended surface water records. *Water Research*, *203*, 117544. https://doi.org/10.1016/j.watres.2021.117544

EPA. (1983). *Methods for chemical analysis of water and wastes*. US Environmental Protection Agency. EPA 600/4-79-020.

Evans, J. S., Murphy, M. A., Holden, Z. A., & Cushman, S. A. (2011). Modeling species distribution and change using Random Forests. In C. A. Drew, Y. F. Wiersma, & F. Huettmann (Eds.), *Predictive species and habitat modeling in landscape ecology: Concepts and applications* (pp. 139–159). Springer.

Goodman, K. J., Baker, M. A., & Wurtsbaugh, W. A. (2011). Lakes as buffers of stream dissolved organic matter (DOM) variability: Temporal patterns of DOM characteristics in mountain stream-lake systems. *Journal of Geophysical Research*, *116*, G00N02. https://doi.org/10.1029/2011jg001709

Green, S. A., & Blough, N. V. (1994). Optical absorption and fluorescence properties of chromophoric dissolved organic matter in natural waters. *Limnology & Oceanography*, *39*(8), 1903–1916. https://doi.org/10.4319/lo.1994.39.8.1903

Greenwell, B. M. (2017). pdp: An R package for constructing partial dependence plots. *The R Journal*, *9*(1), 421–436. Retrieved from https://journal.r-project.org/archive/2017/RJ-2017-016/index.html

Griffin, C. G., Finlay, J. C., Brezonik, P. L., Olmanson, L., & Hozalski, R. M. (2018). Limitations on using CDOM as a proxy for DOC in temperate lakes. *Water Research*, *144*, 719–727. https://doi.org/10.1016/j.watres.2018.08.007

Hayakawa, K., Kojima, R., Wada, C., Suzuki, T., Sugiyama, Y., Kumagi, T., et al. (2016). Distribution and characteristics of ultraviolet absorption and fluorescence of dissolved organic matter in a large lake (Lake Biwa, Japan). *Journal of Great Lakes Research*, *42*(3), 571–579. https://doi.org/10.1016/j.jglr.2016.02.006

He, Y., Song, N., & Jiang, H.-L. (2018). Effects of dissolved organic matter leaching from macrophyte litter on black water events in shallow lakes. *Environmental Science and Pollution Research*, *25*(10), 9928–9939. https://doi.org/10.1007/s11356-018-1267-0

Helms, J. R., Stubbins, A., Ritchie, J. D., Minor, E. C., Kieber, D. J., & Mopper, K. (2008). Absorption spectral slopes and slope ratios as indicators of molecular weight, source, and photobleaching of chromophoric dissolved organic matter. *Limnology & Oceanography*, *53*(3), 955–969. https://doi.org/10.4319/lo.2008.53.3.0955

Hessen, D. O., & Tranvik, L. J. (1998). Aquatic humic matter: From molecular structure to ecosystem stability. In D. O. Hessen, & L. J. Tranvik (Eds.), *Ecological studies: Aquatic humic substances* (pp. 333–343). Springer-Verlag.

Hill, R. A., Weber, M. H., Debbout, R. M., Leibowitz, S. G., & Olsen, A. R. (2018). The Lake-Catchment (LakeCat) dataset: Characterizing landscape features for lake basins within the conterminous USA. *Freshwater Science*, *37*(2), 208–221. https://doi.org/10.1086/697966

Hu, C., Muller-Karger, F. E., & Zepp, R. G. (2002). Absorbance, a(300) and apparent quantum yield: A comment on common ambiguity in the use of these optical concepts. *Limnology & Oceanography*, *47*(4), 1261–1267. https://doi.org/10.4319/lo.2002.47.4.1261

Huguet, A., Vacher, L., Relexans, S., Saubusse, S., Froidefone, J. M., & Parlanti, E. (2009). Properties of fluorescent dissolved organic matter in the Gironde Estuary. *Organic Geochemistry*, *40*(6), 706–719. https://doi.org/10.1016/j.orggeochem.2009.03.002

Juetten, K., Strecker, A. L., Harrison, A., Landram, Z., De Bruyn, W. J., & Clark, C. D. (2022). *Supporting information for chromophoric dissolved organic matter (CDOM) across an elevational gradient from sea level to mountain lakes in the Pacific Northwest [supporting information Tables and figures]* (Vol. 15). Chemistry Faculty and Staff Publications. https://doi.org/10.25710/6x7v-4858. Retrieved from https://cedar.wwu.edu/chemistry_facpubs/15

Kim, J., Kim, Y., Park, S. E., Kim, T.-H., Kim, B.-G., Kang, D.-J., & Rho, T. (2022). Impact of aquaculture on distribution of dissolved organic matter in coastal Jeju Island, Korea, based on absorption and fluorescence spectroscopy. *Environmental Science and Pollution Research*, *29*(1), 553–563. https://doi.org/10.1007/s11356-021-15553-3

Kothawala, D. N., von Wachenfeldt, E., Koehler, B., & Tranvik, L. J. (2012). Selective loss and preservation of lake water dissolved organic matter fluorescence during long-term dark incubations. *Science of the Total Environment*, *433*, 238–246. https://doi.org/10.1016/j.scitotenv.2012.06.029

Laurion, I., Ventura, M., Catalan, J., Psenner, R., & (2000). Attenuation of ultraviolet radiation in mountain lakes: Factors controlling the among- and within-lake variability. *Limnology & Oceanography*, *45*(6), 1274–1288. https://doi.org/10.4319/lo.2000.45.6.1274

Lawaetz, A., & Stedmon, C. A. (2009). Fluorescence intensity calibration using the Raman peak scatter of water. *Applied Spectroscopy*, *63*(8), 936–940. https://doi.org/10.1366/000370209788964548

Li, M., Song, G., & Xie, H. (2022). Bio- and photo-lability of dissolved organic matter in the Pearl River (Zhujiang) estuary. *Marine Pollution Bulletin*, *174*, 113300. https://doi.org/10.1016/j.marpolbul.2021.113300

Liaw, A., & Wiener, M. (2002). Classification and regression by randomForest. *R News*, *2*(3), 18–22.

McKnight, D. M., & Aiken, G. R. (1998). Sources and age of aquatic humus. In D. O. Hessen, & L. J. Tranvik (Eds.), *Ecological studies: Aquatic humic substances* (pp. 9–40). Springer-Verlag.

McKnight, D. M., Boyer, E. W., Westerhoff, P. K., Doran, P. T., Kulbe, T., & Andersen, D. T. (2001). Spectrofluorometric characterization of dissolved organic matter for indication of precursor organic material and aromaticity. *Limnology & Oceanography*, *46*(1), 38–48. https://doi.org/10.4319/lo.2001.46.1.0038

Minor, E. C., Swenson, M. M., Mattson, B. M., & Oyler, A. R. (2014). Structural characterization of dissolved organic matter: A review of current techniques for isolation and analysis. *Environmental Science: Processes & Impacts*, *16*(9), 2064–2079. https://doi.org/10.1039/C4EM00062E

Molot, L., & Dillon, P. J. (1997). Photolytic regulation of dissolved organic carbon in northern lakes. *Global Biogeochemical Cycles*, *11*(3), 357–365. https://doi.org/10.1029/97gb01198

Moran, M. A., & Zepp, R. G. (1997). Role of photoreactions in the formation of biologically labile compounds from dissolved organic matter. *Limnology & Oceanography*, *42*(6), 1307–1316. https://doi.org/10.4319/lo.1997.42.6.1307

Murphy, K. R., Stedmon, C. A., Graeber, D., & Bro, R. (2013). Fluorescence spectroscopy and multi-way techniques. PARAFAC. *Analytical Methods*, *5*(23), 6557–6566. https://doi.org/10.1039/c3ay41160e

Nebbioso, A., & Piccolo, A. (2013). Molecular characterization of dissolved organic matter (DOM): A critical review. *Analytical and Bioanalytical Chemistry*, *405*(1), 109–124. https://doi.org/10.1007/s00216-012-6363-2

Oba, S., Sato, M., Takemasa, I., Monden, M., Matsubara, K., & Ishii, S. (2003). A Bayesian missing value estimation method for gene expression profile data. *Bioinformatics*, *19*(16), 2088–2096. https://doi.org/10.1093/bioinformatics/btg287

Obernosterer, I., & Benner, R. (2004). Competition between biological and photochemical processes in the mineralization of dissolved organic carbon. *Limnology & Oceanography*, *49*(1), 117–124. https://doi.org/10.4319/lo.2004.49.1.0117

Ohno, T. (2002). Fluorescence inner-filtering correction for determining the humification index of dissolved organic matter. *Environmental Science & Technology*, *36*(4), 742–746. https://doi.org/10.1021/es0155276

Olson, M. H., Fischer, J. M., & Hayashi, M. (2021). Temporal dynamics of dissolved organic matter (DOM) in mountain lakes: The role of catchment characteristics. *Canadian Journal of Fisheries and Aquatic Sciences*, *79*(2), 289–299. https://doi.org/10.1139/cjfas-2020-0421

Olson, M. H., Fischer, J. M., Williamson, C. E., Overholt, E. P., & Theodore, N. (2018). Landscape-scale regulators of water transparency in mountain lakes: Implications of projected glacial loss. *Canadian Journal of Fisheries and Aquatic Sciences*, *75*(7), 1169–1176. https://doi.org/10.1139/cjfas-2017-0215

Osburn, C. L., Wigdahl, C. R., Fritz, S. C., & Saros, J. E. (2011). Dissolved organic matter composition and photoreactivity in Prairie Lakes of the U.S. Great Plains. *Limnology & Oceanography*, *56*(6), 2371–2390. https://doi.org/10.4319/lo.2011.56.6.2371

Patel-Sorrentino, N., Mounier, S., & Benaim, J. Y. (2002). Excitation-emission matrix to study pH influence on organic matter fluorescence in the Amazon basin rivers. *Water Research*, *36*, 2571–2581.

R Core Team. (2020). *R: A language and environment for statistical computing*. R Foundation for Statistical Computing. Retrieved from https://www.R-project.org/

Rantala, M. V., Nevalainen, L., Rautio, M., Galkin, A., & Luoto, T. P. (2016). Sources and controls of organic carbon in lakes across the subarctic treeline. *Biogeochemistry*, *129*(1–2), 235–253. https://doi.org/10.1007/s10533-016-0229-1

Rose, K. C., Williamson, C. E., Kissman, C. E. H., & Saros, J. E. (2015). Does allochthony in lakes change across an elevation gradient? *The Ecologist*, *96*(12), 3281–3291. https://doi.org/10.1890/14-1558.1

Sobek, S., Tranvik, L. J., Prairie, Y. T., Kortelainen, P., & Cole, J. J. (2007). Patterns and regulation of dissolved organic carbon: An analysis of 7,500 widely distributed lakes. *Limnology & Oceanography*, *52*(3), 1208–1219. https://doi.org/10.4319/lo.2007.52.3.1208

Song, K., Li, S., Wen, Z., Lyu, L., & Shang, Y. (2019a). Characterization of chromophoric dissolved organic matter in lakes across the Tibet-Qinghai Plateau using spectroscopic analysis. *Journal of Hydrology*, *579*, 124–190. https://doi.org/10.1016/j.jhydrol.2019.124190

Song, K., Shang, Y., Wen, Z., Jacinthe, P.-A., Liu, G., Lyu, L., & Fang, C. (2019). Characterization of CDOM in saline and freshwater lakes across China using spectroscopic analysis. *Water Research*, *150*, 403–417. https://doi.org/10.1016/j.watres.2018.12.004

Stedmon, C. A., Markager, S., & Bro, S. (2003). Tracing dissolved organic matter in aquatic environments using a new approach to fluorescence spectroscopy. *Marine Chemistry*, *82*(3–4), 219–254. https://doi.org/10.1016/s0304-4203(03)00072-0

Su, Y., Chen, F., & Liu, Z. (2015). Comparison of optical properties of chromophoric dissolved organic matter (CDOM) in alpine lakes above or below treeline: Insights into sources of CDOM. *Photochemical and Photobiological Sciences*, *14*, 1047–1309.

Tank, S. E., Lesack, L. F. W., Gareis, J. A. L., Osburn, C. L., & Hesslein, R. H., (2011). Multiple tracers demonstrate distinct sources of dissolved organic matter to lakes of the Mackenzie Delta, western Canadian Arctic. *Limnology and Oceanography*, *56*(4), 1297–1309. https://doi.org/10.4391/lo.2011.56.4.1297

Thornton, D. C. O. (2014). Dissolved organic matter (DOM) release by phytoplankton in the contemporary and future ocean. *European Journal of Phycology*, *49*(1), 20–46. https://doi.org/10.1080/09670262.2013.875596

Tranvik, L. J., Downing, J. A., Cotner, J. B., Loiselle, S. A., Striegl, R. G., Ballatore, T. J., et al. (2009). Lakes and reservoirs as regulators of carbon cycling and climate. *Limnology & Oceanography*, *54*(6part2), 2298–2314. https://doi.org/10.4319/lo.2009.54.6_part_2.2298

United States Geological Survey (USGS). (2020). USGS watershed boundary dataset (WBD) for 2-digit Hydrologic Unit. U.S. Geological Survey. Retrieved from https://www.usgs.gov/core-science-systems/ngp/national-hydrography/access-national-hydrography-productsRefstyled

Urban, N. R., Auer, M. T., Green, S. A., Lu, X., Apul, D. S., Powell, K. D., & Bub, L. (2005). Carbon cycling in lake superior. *Journal of Geophysical Research*, *110*(C6), C06S90. https://doi.org/10.1029/2003JC00230

Vila Dupla, M. (2022). Characterization of cDOM in the Elkhorn Slough estuary using EEM spectroscopy and its potential for macrophyte monitoring. *Journal of Marine Systems*, *226*, 103661.

Vione, D., Minella, M., Maurino, V., & Minero, C. (2014). Indirect photochemistry in sunlit surface waters: Photoinduced production of reactive transient species. *Chemistry - A European Journal*, *20*(34), 10590–10606. https://doi.org/10.1002/chem.201400413

von Wachenfeldt, E., Sobek, S., Bastviken, D., & Tranvik, L. J. (2008). Linking allochthonous dissolved organic matter and boreal lake sediment carbon sequestration: The role of light-mediated flocculation. *Limnology & Oceanography*, *53*(4), 2416–2426.

Wang, X., Chen, R. F., Cable, J. E., & Cherrier, J. (2014). Leaching and microbial degradation of dissolved organic matter from salt marsh plants and seagrasses. *Aquatic Sciences*, *76*, 595–609. https://doi.org/10.1007/s00027-014-0357-4

Weishaar, J. L., Aiken, G. R., Bergamaschi, B. A., Fram, M. S., Fujii, R., & Mopper, K. (2003). Evaluation of specific ultraviolet absorbance as an indicator of the chemical composition and reactivity of dissolved organic carbon. *Environmental Science & Technology*, *37*(20), 4702–4708. https://doi.org/10.1021/es030360x

Weiwei, L., Xin, Y., Keqiang, S., Baohua, Z., & Guang, G. (2018). Unraveling the sources and fluorescence compositions of dissolved and particulate organic matter (DOM and POM) in Lake Taihu, China. *Environmental Science and Pollution Research*, *26*(4), 4027–4040. https://doi.org/10.1007/s11356-018-3873-2

Winn, N., Williamson, C. E., Abbitt, A., Rose, K., Renwick, W., Henry, M., & Saros, J. (2009). Modeling dissolved organic carbon in subalpine and alpine lakes with GIS and remote sensing. *Landscape Ecology*, *24*(6), 807–816. https://doi.org/10.1007/s10980-009-9359-3

Xenopoulos, M. A., Lodge, D. M., Frentress, J., Kreps, T. A., Bridgham, S. D., Grossman, E., & Jackson, C. J. (2003). Regional comparisons of watershed determinants of dissolved organic carbon in temperate lakes from the Upper Great Lakes region and selected regions globally. *Limnology & Oceanography*, *48*(6), 2321–2334. https://doi.org/10.4319/lo.2003.48.6.2321

Xiao, M., Wu, F., Yi, Y., Han, Z., & Wang, Z. (2019). Optical properties of dissolved organic matter and controlling factors in Dianchi Lake waters. *Water*, *11*(10), 1967. https://doi.org/10.3390/w11101967

Xu, J., Wang, Y., Gao, D., Yan, Z., Gao, C., & Wang, L. (2017). Optical properties and spatial distribution of chromophoric dissolved organic matter (CDOM) in Poyang Lake, China. *Journal of Great Lakes Research*, *43*(4), 700–709. https://doi.org/10.1016/j.jglr.2017.06.002

Yamashita, Y., & Jaffe, R. (2008). Characterizing the interactions between trace metals and dissolved organic matter using excitation-emission matrix and parallel factor analysis. *Environmental Science & Technology*, *42*(19), 7374–7379. https://doi.org/10.1021/es801357h

Yao, X., Zhang, Y., Zhu, G., Qin, B., Feng, L., Cai, L., & Gao, G. (2011). Resolving the variability of CDOM fluorescence to differentiate the sources and fate of CDOM in Lake Taihu and its tributaries. *Chemosphere*, *82*(2), 145–155. https://doi.org/10.1016/j.chemosphere.2010.10.049

Ylostalo, P., Kallio, K., & Seppala, J. (2014). Absorption properties of in-water constituents and their variation among various lake types in the boreal region. *Remote Sensing of Environment*, *148*, 190–205. https://doi.org/10.1016/j.rse.2014.03.023

Zhang, Y. L., & Qin, B. Q. (2007). Variations in spectral slope in Lake Taihu, a large subtropical shallow lake in China. *Journal of Great Lakes Research*, *33*(2), 483–496. https://doi.org/10.3394/0380-1330(2007)33[483:vissil]2.0.co;2

Zhang, Y. L., Quin, B., Zhu, G., Zhang, L., & Yang, L. (2007). Chromophoric dissolved organic matter (CDOM) absorption characteristics in relation to fluorescence in Lake Taihu, China, a large shallow subtropical lake. *Hydrobiology*, *581*(1), 43–52. https://doi.org/10.1007/s10750-006-0520-6

Zhang, Y. L., Yin, Y., Feng, L., Zhu, G., Shi, Z., Liu, X., & Zhang, Y. (2011). Characterizing chromophoric dissolved organic matter in Lake Tianmuhu and its catchment basin using excitation-emission matrix fluorescence and parallel factor analysis. *Water Research*, *45*(16), 5110–5122. https://doi.org/10.1016/j.watres.2011.07.014

Zhang, Y. L., Yin, Y., Liu, X., Shi, S., Feng, L., Liu, M., et al. (2011). Spatial-seasonal dynamics of chromophoric dissolved organic matter in Lake Taihu, a large eutrophic shallow lake in China. *Organic Geochemistry*, *42*(5), 510–519. https://doi.org/10.1016/j.orggeochem.2011.03.007

Zhang, Y. L., Zhang, E., Yin, Y., van Dijk, M. A., Feng, L., Shi, Z., et al. (2010). Characteristics and sources of chromophoric dissolved organic matter in lakes of the Yungui Plateau, China, differing in trophic state and altitude. *Limnology & Oceanography*, *55*(6), 2645–2659. https://doi.org/10.4391/lo.2010.55.6.2645

Zhang, Y. L., Zhou, L., Zhou, Y., Zhang, L., Yao, X., Shi, K., et al. (2021). Chromophoric dissolved organic matter in inland waters: Present knowledge and future challenges. *Science of the Total Environment*, *759*, 143550. https://doi.org/10.1016/j.scitotenv.2020.143550

Zhao, Y., Song, K., Wen, Z., Fang, C., Shang, Y., & Lv, L. (2017). Evaluation of CDOM sources and their links with water quality in the lakes of Northeast China using fluorescence spectroscopy. *Journal of Hydrology*, *550*, 80–91. https://doi.org/10.1016/j.jhydrol.2017.04.027

Zhou, Z., Guo, L., & Minor, E. C. (2016). Characterization of bulk and chromophoric dissolved organic matter in the Laurentian Great Lakes during summer 2013. *Journal of Great Lakes Research*, *42*(4), 789–801. https://doi.org/10.1016/j.jglr.2016.04.006

Zsolnay, A., Baigar, E., Jimenez, M., Steinweg, B., & Saccomandi, F. (1999). Differentiating with fluorescence spectroscopy the sources of dissolved organic matter in soils subjected to drying. *Chemosphere*, *38*(1), 45–50. https://doi.org/10.1016/s0045-6535(98)00166-0